

Very Long Baseline Interferometry Experiment on Giant Radio Pulses of Crab Pulsar toward Fast Radio Burst Detection

K. Takefuji¹, T. Terasawa², T. Kondo¹, R. Mikami², H. Takeuchi³, H. Misawa⁴, F. Tsuchiya⁴, H. Kita⁴ and M. Sekido¹
takefuji@nict.go.jp

ABSTRACT

We report on a very long baseline interferometry (VLBI) experiment on giant radio pulses (GPs) from the Crab pulsar in the radio 1.4 to 1.7 GHz range to demonstrate a VLBI technique for searching for fast radio bursts (FRBs). We carried out the experiment on 26 July 2014 using the Kashima 34 m and Usuda 64 m radio telescopes of the Japanese VLBI Network (JVN) with a baseline of about 200 km. During the approximately 1 h observation, we could detect 35 GPs by high-time-resolution VLBI. Moreover, we determined the dispersion measure (DM) to be 56.7585 ± 0.0025 on the basis of the mean DM of the 35 GPs detected by VLBI. We confirmed that the sensitivity of a detection of GPs using our technique is superior to that of a single-dish mode detection using the same telescope.

Subject headings: Data Analysis and Technique : Supernovae – Crab Pulsar

1. Introduction

Lorimer et al. (2007) reported an interesting burst phenomenon, the so-called fast radio bursts (FRBs), which comprised a single impulse of 30 Jy with a frequency-dependent dispersion having a dispersion measure (DM) of 375 pc cm^{-3} , in wide-field pulsar surveys using the 13-beam, 1.4 GHz receiver at the Parkes radio telescope. This large DM with a Galactic latitude of -42° indicates that the pulse has a cosmological origin at $z \sim 0.3$. After the discovery of FRBs, some FRBs were detected with the Parkes radio telescope (Lorimer et al. 2007, Thornton et al.

2013, Burke-Spolaor and Bannister 2014) and FRB110523 detected with the Green Bank telescope revealed Faraday rotation (Masui et al. 2015), and FRB121102 detected with the Arecibo radio telescope (Spitler et al. 2014). Spitler et al. (2016) reported the detection of ten additional bursts, which have dispersion measures and sky positions consistent with the original burst of FRB121102, using the Arecibo telescope. Although most reported FRBs were discovered later in archival data, FRB150418 was recently detected in real-time by the Parkes 64 m radio telescope, which triggered follow-up observations at wavelengths of 5.5 GHz and 7.5 GHz by the Australia Telescope Compact Array (ATCA) 2 h after the event and optical observation by Suprime-Cam on the 8.2 m Subaru telescope within the ~ 1 arcsec positional uncertainty derived from the ATCA image in the following two days (Keane et al. 2016). Keane et al. (2016) identified an elliptical galaxy as the host galaxy of FRB150418, whose redshift was measured to be $z = 0.492 \pm 0.008$ with a fading radio transient lasting ~ 6 days after the

¹National Institute of Information and Communications Technology, 893-1 Hirai, Kashima, Ibaraki 314-8501, Japan.

² Institute for Cosmic Ray Research, The University of Tokyo, Kashiwa, Chiba 277-8582, Japan

³ Institute of Space and Astronautical Science, Japan Aerospace Exploration Agency, Sagami-hara, Kanagawa 252-5210, Japan

⁴ Planetary Plasma and Atmospheric Research Center, Tohoku University, Sendai, Miyagi 980-8578, Japan

event. Exciting FRB astronomy is now underway. However, in order to understand the property of FRBs astrophysically, a large number of FRB events, multi-frequency counterpart identification, and host identification are required.

Astronomical and geodetic very long baseline interferometry (VLBI) (e.g., Very Long Baseline Array (VLBA), European VLBI Network (EVN), The Australian Long Baseline Array (LBA), and East-Asia VLBI Network (EAVN)) is routinely performed throughout the year while observing almost the entire sky. Thus, if we detect FRBs by VLBI observations, the number of detections could be increased and the detection by VLBI could provide essential scientific information in terms of FRB localization. However, these VLBI observations have not been dedicated to finding only FRBs. We should perform these observations as a by-product without disturbing the main observations. Wayth et al. (2011) carried out an experiment called V-FASTR to perform a blind search for fast transient radio signals using VLBA. Since they searched for FRBs using several single dishes operated in parallel, it was not a "true" VLBI experiment. If a survey of FRBs is carried out by VLBI, the sensitivity must be higher than that of single-dish detection methods using same telescopes. In order to explore the possibilities of FRB detection by VLBI, we carried out a true VLBI experiment by observing the Crab pulsar, which often produces very large pulses, so-called giant radio pulses (hereafter GPs). Currently over 2000 pulsars have been found, although only a handful of them have been found to emit GPs (Knight 2006). Individual GPs from the Crab pulsar reach brightness temperatures of at least 10^{32} K (Cordes et al. 2004), which do not resolve the narrowest pulses. GPs are known to reach 10^{37} K in nanosecond-resolution observations (Hankins et al. 2003). Since the GPs from the Crab pulsar are dispersed for a DM of about 56.8 pc cm^{-3} , a de-dispersion process is required to reconstruct a sharp pulse. Thus, since the GPs from the Crab pulsar have a short time scale and a dispersed pulse, they have similar characteristics to FRBs. Rudnitskiy et al. (2015) reported a preliminary VLBI result for a GP from the Crab pulsar with Radioastron at space-ground baselines, and the correlation for space-ground baselines was found in four sessions at 18 cm. They estimated

several parameters to obtain primary information about scattering effects in the interstellar medium using a changing correlation amplitude that depended on the baseline projection. In the field of transient radio phenomena, it is necessary to announce a detection as soon as possible. Normally, we do not perform searches of baseband data because the recording data rate is too high to process. A feasible procedure for searching for transient impulses at a high speed is required. As reported in this paper, we found correlations of GPs from the Crab pulsar by VLBI. The correlations appeared as sharp peaks in the cross-spectrum, which we will use as a trigger for an alert signal without disturbing the correlation process. Here, we report the VLBI observation of the Crab pulsar and determine the DM by newly developed high-time-resolution VLBI.

2. Observations

We carried out the 1 h VLBI experiment from 23h UTC on 26 July 2014 using the Kashima 34 m and Usuda 64 m radio telescopes, the latter having the largest antenna in Japan. The baseline length between the two antennas is about 200 km. We used the L-band and the right-hand circular polarization of both radio telescopes. The L-band receiver of the Kashima 34 m radio telescope has cooled band-pass filters, whose pass-bands have frequency ranges of 1405 to 1440 MHz and 1600 to 1720 MHz, installed before the low-noise amplifier to suppress external interference. The system equivalent flux density (SEFD) of the Kashima 34 m and Usuda 64 m radio telescopes are typically 400 and 100 Jy, respectively.

The downconverted received signal of the L-band receiver was transferred to an observation room. Then, the intermediate signal with a frequency below 512 MHz was digitally baseband-converted (DBBC) and four-bit-recorded at a sampling rate of 64 MHz using an ADS3000+ digital sampler, which has 16 DBBC channels (Takefuji et al. 2010). The 32 MHz frequency ranges of the seven recording channels were tuned for the bandwidths of 1400 to 1432 MHz, 1411 to 1443 MHz, 1570 to 1602 MHz, 1602 to 1634 MHz, 1634 to 1666 MHz, 1666 to 1698 MHz, and 1698 to 1730 MHz. However, with the seven channels fully covered with the above pass-bands of the

L-band receiver, we did not use the other DBBC channels. The basebands of the seven channels were digitally recorded at the Nyquist rate with a 64 MHz sampling speed. Before the Crab pulsar observation, we observed quasar 0552+398 for 30 s from 23:04 on 26 July 2014 to determine the clock offset between the seven channels.

3. Results

Firstly, we performed a correlation using a GICO3 software correlator (Oyama et al. 2012) to measure the clock offset, and thus obtained the correlation of quasar 0552+398 between Kashima 34 m and Usuda 64 m. The signal-to-noise ratio (SNR) of each channel became over 150 with 30 s integration. The measured clock offsets for the second to the seventh channels relative to the delay in the first channel were 2.078 ns, 18.751 ns, 22.249 ns, 23.007 ns, 21.987 ns, and 21.833 ns, respectively.

Next, we performed the de-dispersion only for the first channel of Kashima 34 m with the frequency range of 1400 to 1432 MHz to find GP candidates. Figure 1 shows the obtained Crab pulsar phase plotted against time during the 1 h observation. We used a DM of 56.78 pc cm⁻³ referenced by the Jodrell Bank monthly ephemeris of the Crab pulsar¹ (Lyne et al. 1993) and 1 μ s integration. As a result, we found 71 GPs with an SNR above 18. The strongest GP during the observation had an SNR of 504 and was observed at 23:31:22.11 on 26 July 2014. Next, we will perform the VLBI correlation on the baseband data of the 71 GPs found by single-dish observation.

Now, we will explain the procedure of VLBI correlation for GPs with a GICO3 software correlator. When we process normal VLBI data with digital FX-type spectrometers, Fourier transformation and multiplication are applied to the data to obtain a power spectrum of the signal. However, GPs and FRBs, which have swept-frequency characteristics, become smeared pulses after performing the integration. To avoid smeared pulses, we skipped the integration process in GICO3 to realize a high time resolution for processing a GP signal. We performed this high-time-resolution process on the strongest GP from the seventh dig-

itized baseband data as an example.

Figure 2 shows the correlation of the strongest GP in both the time and frequency domains with 1024 Fourier lengths per 32 MHz bandwidth (62.5 kHz resolution). A sharp peak with SNR of 35 appears in the right-side cross-spectrum in Figure 2 at 23:31:22.118672 from a single Fourier period of 16 μ s (1024 Fourier lengths in 64 MHz sampling). In contrast to the frequency domain, although we observed no correlation from a single Fourier period in the time domain, we needed more time in the case of 400 μ s integration to accumulate 25 Fourier bins to find the weak and broad correlation on the left of Figure 2 at 23:31:22.1212. Such a weak and broadened signal with SNR of 4.8 in the time domain would be difficult and ineffective to search for. However, sharp peaks that appeared in the Fourier domain could be used as a trigger for an alert signal without disturbing the correlation process.

For the strongest GP, we next stacked all Fourier bins in which the GP existed for about 40 ms in all seven channels. Although the amount of cross-spectrum data became huge (about 72 MB in only 40 ms), we only extracted the peak frequency and its amplitude to reduce the amount of data. As described previously, the maximum time difference between the seven channels was 23 ns. Since this is smaller than the single Fourier length of 16 μ s, we ignored the time differences. Then, we stacked the extracted peaks from every Fourier bin as shown in Figure 3. In total, 22,000 (50 ms / 16 μ s \times 7 bands) data points were included in the figure. A GP curve originating from the dispersed delay caused by the interstellar medium and an artificial signal at 1620 MHz possibly from a Japanese communication satellite were observed. However, an artificial signal with a specific frequency can be clearly distinguished and easily removed.

Next, we estimated the DM from the dispersed curve in Figure 3. The observation equation with respect to the arrival time of the GP, $\tau(f)$, is,

$$\tau(f) = \frac{e^2}{2\pi m_e c} \frac{DM}{f^2} + t_0, \quad (1)$$

where e is the electron charge, m_e is the electron mass, c is the speed of light, and t_0 is the arrival time at the highest frequency. Although it was easy to estimate the unknown parameters DM

¹<http://www.jb.man.ac.uk/pulsar/crab.html>

and t_0 from Figure 3 by the least-squares method (LSM) using a standard gnuplot, the other weaker GPs could not be fitted using the gnuplot. Thus, we wrote an automated fitting program with the C++ template library Eigen² for linear algebra. The functions of our LSM program are as follows:

- Calculating and removing the interference in specific frequency migration by stacking at every frequency resolution automatically.
- Iterative fitting by removing noise outside 3σ from the GP curve and narrowing the time (initially 50 ms) by 99% in slow steps to prevent a local minimum and calculating the chi-square value.
- Estimating DM and t_0 when the chi-square value becomes within 1 ± 0.01 .

We differentiate equation (1) with respect to the frequency f . $\tau(f)$ has an uncertain value, which we used as the weight for the chi-square calculation, with regard to the observation frequency,

$$\frac{d\tau(f)}{df} = -\frac{e^2}{\pi m_e c} \frac{DM}{f^3} \quad (2)$$

$$= -2\frac{\tau(f)}{f}. \quad (3)$$

Finally, we performed the previous process, which includes a correlation, stacking the peaks, and fitting, routinely for the 71 GPs already found by single-dish observation and obtained a DM of 56.754 to 56.770 from the 35 GPs detected by VLBI. The mean value of the DM was estimated to be 56.7620 ± 0.0025 , as shown in Figure 4. The final DM considering the Doppler effects of the Earth's revolution is 56.7585 ± 0.0025 . Our DM estimated by VLBI is 2σ close to 56.7632, the value obtained on 14 July 2014 from the Jodrell Bank Crab pulsar monthly ephemeris. This small difference is caused by the fact that the DM is observed to change with time for many pulsars because of solar wind (e.g., You et al. 2007), and the movements of the pulsar, the Earth, and the interstellar medium (e.g., Keith et al. 2013). You et al. (2007) reported that a solar wind contributes ~ 100 ns at 1400 MHz for sources within 60° of the Sun and $\sim 1 \mu\text{s}$ for sources within 7° of the Sun.

Since we observed the Crab pulsar within about 45° of the Sun, we assume that the solar wind contributes approximately 250 ns by interpolating the above relationship and taking the log of the times, which corresponds to a DM variation on the order of 10^{-3} .

4. Discussion

Since the numbers of GPs detected by VLBI observation 35 was less than the 71 GPs ($\text{SNR} > 18$) extracted from only a de-dispersed single 32 MHz channel, the VLBI technique that we applied is disadvantageous compared with the single-dish observation. This is because we used only one peak frequency in the $16 \mu\text{s}$ cross-spectrum bin, which had a total of 1024 data in this case. For the sake of comparison between single-dish and VLBI observation, we performed the same VLBI process for the 71 GPs obtained using a single dish (Kashima 34 m or Usuda 64 m). In the VLBI, we performed our processing on the cross-spectrum. In contrast, we performed the processing on the power spectra of both Kashima and Usuda for the single-dish observations. We counted the GP residuals after fitting from 1400 to 1730 MHz as the comparison method. The result is shown in Table 1. For example, the strongest GP at 23:31:22 in line 17 has 1085 GP residuals for the case of VLBI. However, the two single-dish observations found 842 and 935 GP residuals for Kashima and Usuda, respectively. Thus, the results obtained by VLBI were superior to those obtained by the single-dish observation, and were on average 1.6 times higher. Since the VLBI result in the first row in the table existed, some pointing error might have occurred in the case of Usuda 64 m. This VLBI result allows us to distinguish signals from the sky from local interference. For example, some artificial impulses are known to be formed as swept-frequency-dependent signals, which are very similar to FRBs (Burke-Spolaor et al. 2011, Petroff et al. 2015). Since these locally emitted signals are not subjected to interference over a 100 km baseline, we assume that these interferences could be easily neglected by this VLBI technique. In brief, the sensitivity of VLBI is given by

$$\text{SNR} = \frac{F}{\sqrt{\text{SEFD}_1} \sqrt{\text{SEFD}_2}} \sqrt{2BT}, \quad (4)$$

²<http://eigen.tuxfamily.org>

where F is the flux density, $SEFD_1$ and $SEFD_2$ are the SEFDs of the two antennas, $2B$ is the Nyquist sampling speed, and T is the integration time. In our case, the sampling speed $2B$ was 64 MHz and T was 16 μ s. If we determine SNR as a threshold for searching for the peak to be 18, the sensitivity from equation (4) becomes 79.5 Jy as a snapshot, such as right figure in Figure 2. If we integrate the whole 150 MHz on seven channels in our VLBI, the sensitivity becomes 30.1 Jy. Thus, we will perform the de-dispersion on the cross spectrum to acquire better sensitivity as a next study.

Toward the detection of FRBs by VLBI, we propose that all institutes and universities with radio telescopes should observe the same area of the sky and record data while synchronizing the frequency bandwidth during vacant time. If FRBs occur and such data are obtained, we can apply our VLBI technique to detect them. This will increase the detection of FRBs and we can determine the exact localization of the FRBs. Moreover, we normally only search for peaks in the time domain for geodetic and astronomical VLBI, especially for continuum sources. On the basis of our results, we propose that peaks should also be searched for in the frequency domain. Normally we perform correlation by Fourier transforming the data of two stations and multiplying the two spectra to form a cross spectrum. The largest load in the correlation process is the fast Fourier transform (FFT). After every FFT, a peak search in the frequency domain is performed. If we define N as the Fourier length, the processing costs of a simple radix-2 FFT and the linear search are $N \log_2 N$ and N , respectively. In our case, we used 1024 Fourier lengths for a 32 MHz bandwidth (62.5 kHz resolution). This is expected to increase the processing time by 10% as a result of adding a linear search for a peak in the correlation. If we perform the correlation at a rather coarse frequency resolution of 1 MHz as general VLBI processing, the processing time is increased by 20%. If we change the general VLBI processing ($N=32$) to high-time-resolution VLBI ($N=1024$), the processing time is increased by 220%. However, the increase in processing time for the high-time-resolution VLBI will be cancelled out by the recent progress in computers.

5. Summary

We carried out a high-time-resolution VLBI experiment on GPs from the Crab pulsar using the Kashima 34 m and Usuda 64 m radio telescopes in the 1.4 to 1.7 GHz range. We obtained a sharp correlation in the case of 16 μ s integration in the frequency domain after determining the clock offset between two antennas. We also obtained the DM of the GPs from a curve obtained by stacking peaks from every cross-spectrum. Then, we estimated the DM to be 56.7585 ± 0.0025 from the 35 detected GPs. The technique we applied has the potential to detect FRBs.

REFERENCES

- Burke-Spolaor, S., M. Bailes, R. Ekers, J.-P. Macquart, and F. Crawford, III (2011). Radio Bursts with Extragalactic Spectral Characteristics Show Terrestrial Origins. *The Astrophysical Journal*.
- Burke-Spolaor, S. and K. W. Bannister (2014). The Galactic Position Dependence of Fast Radio Bursts and the Discovery of FRB011025. *The Astrophysical Journal*.
- Cordes, J. M., N. D. R. Bhat, T. H. Hankins, M. A. McLaughlin, and J. Kern (2004). The Brightest Pulses in the Universe: Multifrequency Observations of the Crab Pulsar’s Giant Pulses. *The Astrophysical Journal*.
- Hankins, T. H., J. S. Kern, J. C. Weatherall, and J. A. Eilek (2003). Nanosecond radio bursts from strong plasma turbulence in the Crab pulsar. *Nature*.
- Keane, E. F., S. Johnston, S. Bhandari, E. Barr, N. D. R. Bhat, M. Burgay, M. Caleb, C. Flynn, A. Jameson, M. Kramer, E. Petroff, A. Possenti, W. van Straten, M. Bailes, S. Burke-Spolaor, R. P. Eatough, B. W. Stappers, T. Totani, M. Honma, H. Furusawa, T. Hattori, T. Morokuma, Y. Niino, H. Sugai, T. Terai, N. Tominaga, S. Yamasaki, N. Yasuda, R. Allen, J. Cooke, J. Jencson, M. M. Kasliwal, D. L. Kaplan, S. J. Tingay, A. Williams, R. Wayth, P. Chandra, D. Perrodin, M. Berezina, M. Mickaliger, and C. Bassa (2016). The host galaxy of a fast radio burst. *Nature*.

- Keith, M. J., W. Coles, R. M. Shannon, G. B. Hobbs, R. N. Manchester, M. Bailes, N. D. R. Bhat, S. Burke-Spolaor, D. J. Champion, A. Chaudhary, A. W. Hotan, J. Khoo, J. Kocz, S. Osłowski, V. Ravi, J. E. Reynolds, J. Sarkissian, W. van Straten, and D. R. B. Yardley (2013). Measurement and correction of variations in interstellar dispersion in high-precision pulsar timing. *Monthly Notices of the Royal Astronomical Society*.
- Knight, H. S. (2006). Observational Characteristics of Giant Pulses and Related Phenomena. *Chinese Journal of Astronomy and Astrophysics Supplement*.
- Lorimer, D. R., M. Bailes, M. A. McLaughlin, D. J. Narkevic, and F. Crawford (2007). A Bright Millisecond Radio Burst of Extragalactic Origin. *Science*.
- Lyne, A. G., R. S. Pritchard, and F. Graham-Smith (1993). Twenty-Three Years of Crab Pulsar Rotational History. *Monthly Notices of the Royal Astronomical Society*.
- Masui, K., H.-H. Lin, J. Sievers, C. J. Anderson, T.-C. Chang, X. Chen, A. Ganguly, M. Jarvis, C.-Y. Kuo, Y.-C. Li, Y.-W. Liao, M. McLaughlin, U.-L. Pen, J. B. Peterson, A. Roman, P. T. Timbie, T. Voytek, and J. K. Yadav (2015). Dense magnetized plasma associated with a fast radio burst. *Nature*.
- Oyama, T., Y. Kono, S. Suzuki, S. Mizuno, T. Bushimata, T. Jike, N. Kawaguchi, H. Kobayashi, and M. Kimura (2012). New VLBI Observing System 'OCTAVE-Family' to Support VDIF Specifications with 10 GigaE for VERA, JVN, and Japanese e-VLBI (OCTAVE). In D. Behrend and K. D. Baver (Eds.), *Seventh General Meeting (GM2012) of the international VLBI Service for Geodesy and Astrometry (IVS), held in Madrid, Spain, March 4-9, 2012, Eds.: D. Behrend and K.D. Baver, National Aeronautics and Space Administration*.
- Petroff, E., E. F. Keane, E. D. Barr, J. E. Reynolds, J. Sarkissian, P. G. Edwards, J. Stevens, C. Brem, A. Jameson, S. Burke-Spolaor, S. Johnston, N. D. R. Bhat, P. C. S. Kudale, and S. Bhandari (2015). Identifying the source of perytons at the Parkes radio telescope. *Monthly Notices of the Royal Astronomical Society*.
- Rudnitskiy, A., M. Popov, and V. Soglasnov (2015). Preliminary results of giant pulse investigations from Crab pulsar with Radioastron. *ArXiv e-prints*.
- Spitler, L. G., J. M. Cordes, J. W. T. Hessels, D. R. Lorimer, M. A. McLaughlin, S. Chatterjee, F. Crawford, J. S. Deneva, V. M. Kaspi, R. S. Wharton, B. Allen, S. Bogdanov, A. Brazier, F. Camilo, P. C. C. Freire, F. A. Jenet, C. Karako-Argaman, B. Knispel, P. Lazarus, K. J. Lee, J. van Leeuwen, R. Lynch, S. M. Ransom, P. Scholz, X. Siemens, I. H. Stairs, K. Stovall, J. K. Swiggum, A. Venkataraman, W. W. Zhu, C. Aulbert, and H. Fehrmann (2014). Fast Radio Burst Discovered in the Arecibo Pulsar ALFA Survey. *The Astrophysical Journal*.
- Spitler, L. G., P. Scholz, J. W. T. Hessels, S. Bogdanov, A. Brazier, F. Camilo, S. Chatterjee, J. M. Cordes, F. Crawford, J. Deneva, R. D. Ferdman, P. C. C. Freire, V. M. Kaspi, P. Lazarus, R. Lynch, E. C. Madsen, M. A. McLaughlin, C. Patel, S. M. Ransom, A. Seymour, I. H. Stairs, B. W. Stappers, J. van Leeuwen, and W. W. Zhu (2016, March). A repeating fast radio burst. *Nature* 531, 202–205.
- Takefuji, K., H. Takeuchi, M. Tsutsumi, and Y. Koyama (2010). Next-generation A/D Sampler ADS3000+ for VLBI2010. In R. Navarro, S. Rogstad, C. E. Goodhart, E. Sigman, M. Soriano, D. Wang, L. A. White, and C. S. Jacobs (Eds.), *Sixth International VLBI Service for Geodesy and Astronomy. Proceedings from the 2010 General Meeting, "VLBI2010: From Vision to Reality". February 7-13, 2010. Eds.: D. Behrend and K.D. Baver. NASA/CP 2010-215864*.
- Thornton, D., B. Stappers, M. Bailes, B. Barndell, S. Bates, N. D. R. Bhat, M. Burgay, S. Burke-Spolaor, D. J. Champion, P. Coster, N. D'Amico, A. Jameson, S. Johnston, M. Keith, M. Kramer, L. Levin, S. Milia, C. Ng, A. Possenti, and W. van Straten (2013). A Population of Fast Radio Bursts at Cosmological Distances. *Science*.

Wayth, R. B., W. F. Brisken, A. T. Deller, W. A. Majid, D. R. Thompson, S. J. Tingay, and K. L. Wagstaff (2011). V-FASTR: The VLBA Fast Radio Transients Experiment. *The Astrophysical Journal*.

You, X. P., G. Hobbs, W. A. Coles, R. N. Manchester, R. Edwards, M. Bailes, J. Sarkissian, J. P. W. Verbiest, W. van Straten, A. Hotan, S. Ord, F. Jenet, N. D. R. Bhat, and A. Teoh (2007). Dispersion measure variations and their effect on precision pulsar timing. *Monthly Notices of the Royal Astronomical Society*.

No.	Epoch	Type	SNR	VLBI [count]	KASHIMA [count]	USUDA [count]	Increasing rate
1	23:06:59.509753	MP	82.57	250	599		(0.42)
2	23:11:27.462469	MP	22.14	156		94	(1.66)
3	23:11:34.538977	MP	22.67	226	117	152	1.69
4	23:13:05.148274	MP	20.66	144		97	(1.48)
5	23:13:13.417519	IP	21.34	84		65	(1.29)
6	23:16:40.534982	MP	25.44	94			
7	23:17:52.105830	MP	49.20	290	181	204	1.51
8	23:18:58.622391	MP	21.47	78			
9	23:19:56.478841	MP	34.37	371	197	248	1.68
10	23:21:13.643400	MP	22.77	282	153	150	1.86
11	23:22:04.490966	MP	50.18	281	152	195	1.63
12	23:25:03.081545	MP	28.91	124			
13	23:25:18.885214	MP	38.27	191	104	132	1.63
14	23:26:22.975541	MP	20.29	86	42		(2.05)
15	23:27:08.802507	MP	32.57	240	126	127	1.90
16	23:28:50.632612	MP	68.07	386	245	253	1.55
17	23:31:22.131100	MP	504.1	1085	842	935	1.22
18	23:33:19.394396	MP	22.90	111			
19	23:34:48.352736	MP	47.91	224	138	119	1.75
20	23:35:42.670998	MP	60.83	330	158	221	1.77
21	23:36:18.995826	MP	56.45	138		87	(1.59)
22	23:38:39.542937	MP	29.91	146			
23	23:39:39.704649	IP	33.00	240	125	200	1.52
24	23:40:05.940311	MP	25.08	106		74	(1.43)
25	23:41:25.429876	MP	30.09	152	100	115	1.42
26	23:41:55.992362	MP	51.40	166	73	113	1.83
27	23:42:35.181207	MP	150.5	284		177	(1.60)
28	23:44:59.772031	MP	27.71	116			
29	23:45:12.677827	MP	22.69	256	129	183	1.67
30	23:45:24.437880	MP	85.05	190	110	126	1.61
31	23:46:01.975449	MP	47.22	289	157	188	1.68
32	23:47:42.626430	MP	25.84	268		204	(1.31)
33	23:50:50.921363	MP	24.67	194	92	115	1.89
34	23:51:30.716503	MP	112.1	679	436	549	1.39
35	23:51:58.212767	MP	99.38	860	556	666	1.41

Table 1: Comparison of results obtained by counting GP residuals after fitting from 1400 MHz to 1730 MHz obtained by VLBI and using a single dish (Kashima 34 m and Usuda 64 m). Missing values indicate that we could not estimate the DM within 56.75 to 56.77. The type indicates the main pulse and inter pulse of the Crab pulsar, and the SNR shows a value dedispersed for the first channel of Kashima 34 m with the frequency range of 1400 to 1432 MHz. Most of the VLBI results were about 1.6 times higher than the single-dish observation results.

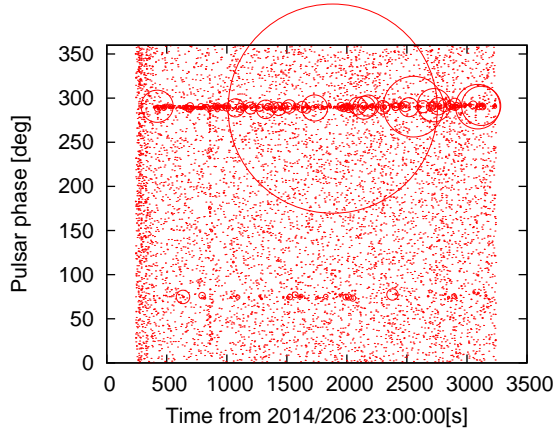


Fig. 1.— Graph of Crab pulsar phase plotted against time during 1 h observation showing main pulse at 290 deg and interpulse at 75 deg. The sizes of the circles represent the SNR for the GPs. We used the first channel of Kashima 34 m with the frequency range of 1400 to 1432 MHz. We performed the dedispersion process using a DM of 56.78 pc cm^{-3} with $1 \mu\text{s}$ integration. When we adjusted the pulsar cycle to 33.6963 ms, the series of GPs aligned with the pulsar phase. The reference point of the pulsar phase is 00:00 on 26 July 2014.

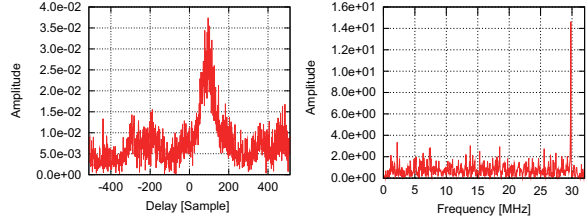


Fig. 2.— VLBI result for the strongest GP from the Crab pulsar on 26 July 2014. The right graph shows the strong GP cross-spectrum in the frequency domain at 1728 MHz in the case of $16 \mu\text{s}$ integration at 23:31:22.118672. The left graph shows the weak and broad GP correlation in the time domain in the case of $400 \mu\text{s}$ integration at 23:31:22.1212.

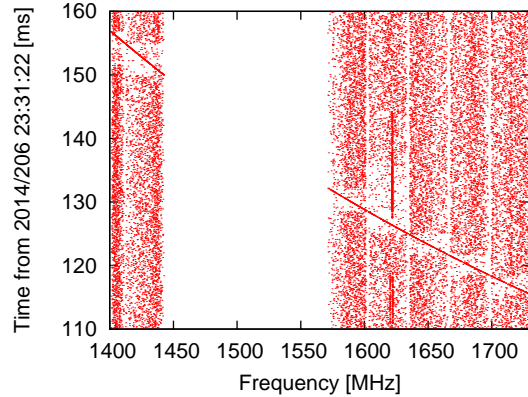


Fig. 3.— Swept-frequency curve of the strongest GP from the Crab pulsar detected from the correlation between Kashima 34 m and Usuda 64 m at 23:31:22 on 26 July 2014, shown as stacked extracted peaks from every $16 \mu\text{s}$ cross-spectra. An artificial signal can be seen at 1620 MHz. However, an artificial signal with a specific frequency can be clearly distinguished and easily removed. We estimated the DM to be 56.7620 ± 0.0003 from the curve.

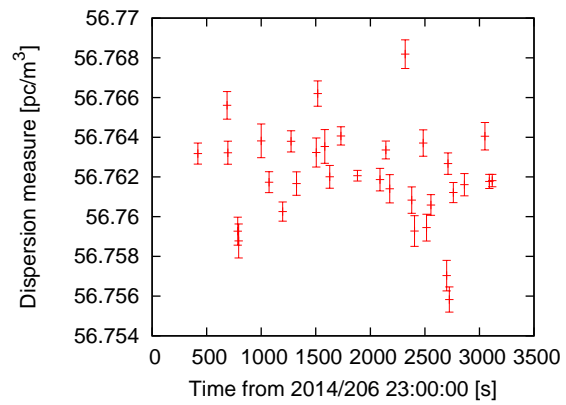


Fig. 4.— Estimated DM from 35 GPs observed by VLBI. The mean DM is 56.7620 ± 0.0025 . The final DM is 56.7585 ± 0.0025 considering the Doppler effects of the Earth's revolution.